PAIWERA – A ROBUST WELLBORE SIMULATOR FOR GEOTHERMAL APPLICATIONS

Peter Franz[1]

[1]Mighty River Power, 283 Vaughan Rd, Rotorua, New Zealand

peter.franz@mightyriver.co.nz

Keywords: *geothermal, wellbore simulator*

ABSTRACT

Wellbore simulators are a key instrument for modeling the behavior and performance of geothermal wells. While a number of wellbore simulators exist for modeling geothermal well behavior they often lack robustness, i.e. they may fail to simulate well behavior under extreme thermodynamic conditions or when using a poor choice of auxiliary parameters. This is usually not a problem when studying a single well case since the modeler can manually guide the simulation. However when simulating reservoir-wellbore-surface facilities in a fully coupled model, this lack of robustness becomes very important since extreme thermodynamic conditions must be accommodated.

To address these important issues MRP has created the wellbore simulator "Paiwera" as an in-house development. Paiwera uses very robust search algorithms internally to accurately determine complex thermodynamic states and auxiliary integration parameters. Since its development Paiwera has been widely used at MRP for a variety of tasks including high-precision wellbore simulation of PTS runs; fully coupled reservoir-wellbore-surface models; batch-mode processing; and Monte Carlo simulations for well performance uncertainty modeling.

This paper gives a brief overview of the most important search strategies used in Paiwera, followed by some application examples.

1. INTRODUCTION

A wellbore simulator is a tool used to simulate the physical conditions that govern the flow of fluid in a geothermal well. The modeler is usually interested in two different simulation results: borehole simulations are a series of profiles (pressure, temperature, etc.) along the wellbore under a fixed operating condition; whereas wellhead simulations make use of multiple borehole simulations to determine the productivity or injectivity of the well.

A number of wellbore simulators are known to exist within the industry; however most of them are either proprietary or non-open code in-house developments, making a thorough comparison difficult. Before the development of Paiwera was started the author had exposure to a variety of GWELL derivatives (Aunzo, Bjornsson, & Bodvarsson, 1991) and to GEOWELL (developed by M. Parini); this can by no means be taken as a comprehensive overview over the existing simulators but others were not available to the author.

Both GWELL and GEOWELL simulators have been used at Mighty River Power. They have proven to be very useful for many wellbore simulation studies; however they require the modeler to enter auxiliary parameters to aid the simulation process. This is a satisfactory solution for many applications but the modeling strategy at MRP is to have fully coupled reservoir/wellbore/surface models for all its fields. It was found that the dynamic changes during reservoir simulation caused these auxiliary parameters to be varied over a wide range to obtain a successful wellbore simulation. Since the user cannot anticipate these auxiliary settings in advance, it was decided that MRP required a more robust wellbore simulator that would determine any auxiliary parameters on its own without user intervention.

This paper describes the most important algorithms used for determining the full operating range of a geothermal production well. Simulation of injection wells follows similar principles and also works well within the Paiwera wellbore simulator; however the algorithms used for injection are more complex and will not be treated here.

2. BACKGROUND

The basis for a wellbore simulator is the conservation of momentum and energy. This results in the following equations describing the change of pressure, dP, and enthalpy, dH, over a section of the wellbore with length dL:

$$\frac{dP}{dL} = \left(\frac{dP}{dL}\right)_h + \left(\frac{dP}{dL}\right)_f + \left(\frac{dP}{dL}\right)_a$$

$$\frac{dH}{dL} = \left(\frac{dH}{dL}\right)_{pot} + \left(\frac{dH}{dL}\right)_a + \left(\frac{dH}{dL}\right)_c$$

where the subscripts h, f and a denote the hydrostatic, friction and acceleration terms in the pressure equation, and potential, acceleration and conductive terms in the enthalpy equation:

$$\left(\frac{dP}{dL}\right)_h = g \cdot \rho_m \cdot \cos\alpha$$

$$\left(\frac{dP}{dL}\right)_f = -\frac{f_m \cdot v_m^2 \cdot \rho_m}{2 \cdot d}$$

$$\left(\frac{dP}{dL}\right)_a = -\rho_m \cdot v_m \cdot \frac{dv_m}{dL}$$

$$\left(\frac{dH}{dL}\right)_{pot} = g \cdot \cos\alpha$$

$$\left(\frac{dH}{dL}\right)_a = -v_m \cdot \frac{dv_m}{dL}$$

$$\left(\frac{dH}{dL}\right)_c = -Q/w$$

Here g denotes the gravitational constant, ρ_m is the mixture density, α is the angle of wellbore inclination, f_m the friction factor, v_m the mixture velocity, d the wellbore diameter, Q

the heat loss term and *w* the mass flow rate. Details to these entities are given elsewhere, e.g. (Hasan & Kabir, 2002).

The mass flow rate *w* is a conserved entity along the wellbore; however at feedzones mass can be exchanged with the reservoir. Typically a linear relationship of the form:

$$\Delta w = const \cdot (P - P_{reservoir})$$

is applied, where the constant describes the productive index and can depend on the thermodynamic conditions present.

For general purposes the component mass fraction vector *X* can be introduced that describes the mass fraction of the flow rate *w* associated with a component. For example *X* could denote the vector:

$$X = (X_{H_2O}, X_{CO_2})$$

for a system containing a mixture of water and carbon dioxide; note that this vector will have unit length.

The friction factor f_m needs to be chosen according to a friction model. A large number of these models, often called pressure drop correlations, exist, e.g. (Hasan & Kabir, 2010), (Hasan & Kabir, 2002), (Peter & Acuna, 2010) and references therein. Paiwera currently only uses the basic homogenous model and the Duns & Ros model (Duns & Ros, 1963). So far these two correlations have proven adequate for a wide range of models; however it would be very easy to implement additional pressure drop correlations at a later stage.

A production wellbore simulation starts at the node containing the lowest feedzone. A suitable initial pressure P_0 is chosen; with this given pressure the amount of fluid entering the wellbore can be determined. Next all necessary thermodynamic quantities in the node can be calculated as functions of (*P, H, X*). After this the remaining entities can be calculated using the model specific parameters, which finally presents the values for *dP/dL* and *dH/dL*. An integration scheme for ordinary differential equations can be used to calculate (*P, H*) in the next node upwards; *X* is a conserved quantity between feedzones. If a feedzone is encountered at a node it can either add or remove fluid from the wellbore, therefore changing the mass flow rate, enthalpy and fluid composition. The simulation ends when the wellhead location is reached.

Wellhead simulations vary the starting pressure P_0 and record (*P, w, H, X*) encountered at the wellhead.

3. IMPLEMENTATION

3.1. ODE Integration Scheme

There exist a multitude of integration schemes for ordinary differential equations (ODE). The most basic one is known as Euler's method:

$$P_{n+1} = P_n + \Delta L \cdot \frac{dP}{dL}$$

While this method is simple to implement it suffers from being a low order method; for example it will methodologically yield too low wellhead pressures for a given simulation, albeit the order of magnitude of its error is usually acceptable. More advanced methods implemented in Paiwera are the Runge-Kutta methods of 4th and 5th order (Press, Teukolsky, Vetterling, & Flannery, 2007). The 5th order with adaptive step size was found useful for single wellbore simulations but produced some undesired scatter in wellhead simulations. The preferred choice ended up being the classical 4th order Runge-Kutta method with fixed step size; the Euler method was still found useful in simulations where speed rather than high accuracy is required (coupled reservoir/wellbores simulations, Monte-Carlo, etc.).

3.2. Thermodynamic Tables

The thermodynamic properties of the fluid need to be taken from thermodynamic tables which have (*P, H, X*) as primary variables. For pure water this does not pose a problem since an adequate system of tables exists ((IAPWS-IF97, 2007) and associated releases).

However if the fluid contains non-condensable gases like CO_2 or salts like NaCl it becomes harder to calculate the fluid properties since most publications give thermodynamic properties as functions of pressure and temperature. Hence there are a couple of different thermodynamic tables implemented in Paiwera which employ root-finding algorithms to determine the temperature of the fluid to then calculate the missing parameters.

For the CO_2 table the enthalpy for a given temperature is calculated by first determining the phase state of the system – liquid, two-phase or gas – following the method lined out by (Aunzo et al., 1991). Once the phase state is determined the enthalpy *H*(*P, T, X*) is calculated as the sum of the enthalpies of steam, liquid water, gaseous CO_2 and dissolved CO_2. For the pure water properties the formulations in (IAPWS-IF97, 2007) are used; for CO_2 the density and viscosity are taken from (Pritchett, Rice, & Riney, 1981), enthalpy from (Sutton & McNabb, 1977) and solubility from (Battistelli, Calore, & Pruess, 1997). The heat of solution is an adapted hybrid function taking formulations from (Carroll, Slupsky, & Mather, 1991), (Ellis & Golding, 1963) and TOUGH2 EOS2 to span the full range [0, 350°C].

The inversion starts by ensuring the problem is properly bounded, i.e. that the enthalpy *H* in the node corresponds to

$$H_{\min}(P, T_{min,}, X_{CO_2}) \leq H \leq H_{\max}(P, T_{max}, X_{CO_2})$$

where T_{min}, T_{max} are table specific, e.g. [0, 350°C]. After this the Van Wijngaarden-Dekker-Brent root-finding method (Press et al., 2007) is used with *T* as the variable to find a sufficiently close solution to *H* = *H*(*P, T, X*). Under normal conditions this method often finds a solution within 4-6 iterations. Once *T* has been determined all remaining thermodynamic properties of the fluid can be calculated.

Two more thermodynamic tables have been implemented, one with NaCl and one with both NaCl and CO_2. These follow a similar approach as given above for CO_2; however the table for NaCl and CO_2 must make a 2D root search over the temperature and the fraction of NaCl dissolved in the liquid phase. Both tables containing NaCl take possible halite precipitation into account; Paiwera allows for solids to be removed from the fluid stream inside the wellbore. This feature can potentially be exploited in the future to model scaling effects.

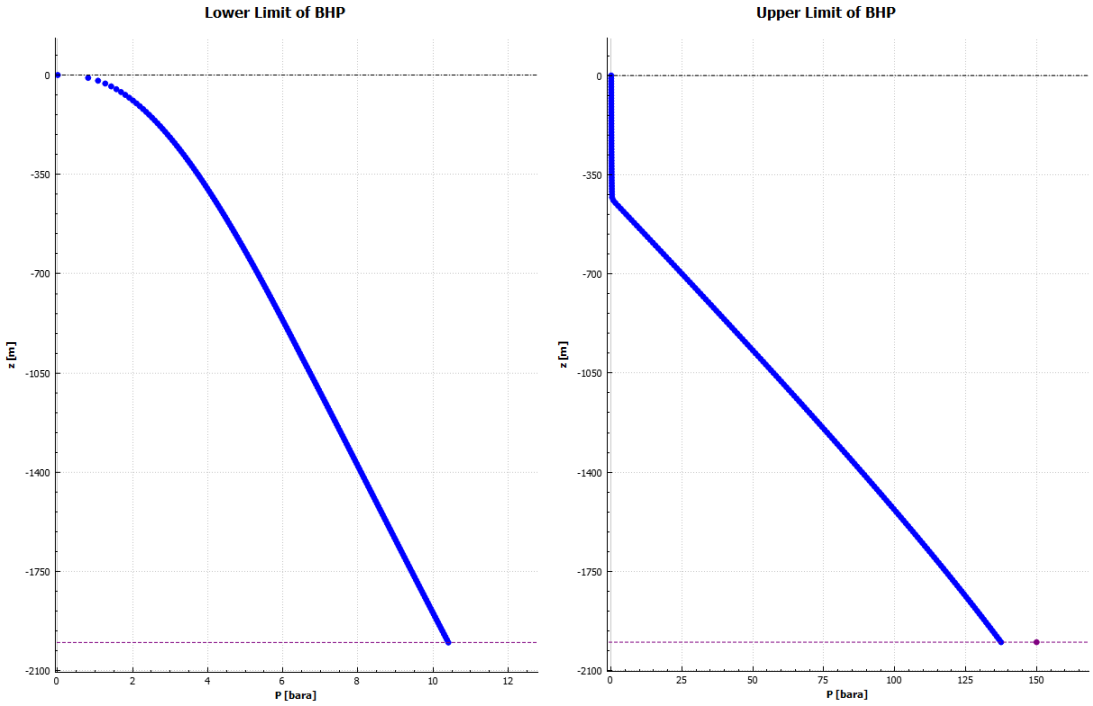

Figure 1: Lower and upper limits for the bottom hole pressure P_0 which still yield valid integration results. The left plot shows the lower limit; any lower value of P_0 would yield negative pressure before reaching the wellhead. The right plot shows the upper limit of P_0 under low flow conditions. The reservoir pressure is at 150 bar; values of $P_0 > 137.4$ bar are not possible since heat loss in the particular example leads to invalid thermodynamic conditions.

3.3. Wellbore Integration Failures

The wellbore simulation needs to be considered as failed if the integration cannot reach the wellhead location. It is very important to establish why the integration failed, since the failure type is needed in the wellhead simulation searches.

In any well with multiple feedzones it is possible to gain or lose mass at a feedzone. If the pressure in the reservoir at a feedzone is higher than the pressure in the well then fluid is gained, else it is lost. It is also possible that a well with a higher internal pressure encounters a feedzone and loses all its fluid to this feedzone. Clearly the integration cannot continue if all fluid to lost to the feedzone; this condition can be termed "total loss".

Another failure mode can happen when the primary variables wander out of the valid range given by the thermodynamic tables. The most prevailing condition is that the pressure becomes zero or negative on the way up in the wellbore; this condition can be termed "invalid".

4. WELLHEAD SIMULATIONS

The methodology described above is sufficient for running single wellbore simulations to generate profiles of the physical entities along the wellbore.

Wellhead simulations consist of a series of single wellbore simulations using different starting pressures P_0. Also in some cases it becomes necessary to alter the start of the integration, L_0. One is therefore interested in the wellhead conditions as a function of the starting parameters, e.g. $P(P_0, L_0)$, $w(P_0, L_0)$, $H(P_0, L_0)$, $X(P_0, L_0)$. The resulting series for the mass flow rate w is usually plotted versus the wellhead pressure to give a "deliverability curve", i.e. the flow rate accessible for production at a given wellhead pressure.

The typical approach for existing wellbore simulators tested was to either set a range and step-size for the starting pressures P_0 and simply integrate upwards collecting the valid results, or to set an initial pressure difference to the reservoir and use a user defined step-size. These methods usually work satisfactorily; however it is quite possible that the range chosen will not find a solution. In particular in cases with multiple feedzones, it is possible that the valid range is very narrow and can be missed by the modeler.

4.2. Single Feedzone Cases

The strategy used to define the valid range for the bottom-hole pressure P_0 is to first find an arbitrary P_0 for which the integration yields a valid result; after this one can use boundary search strategies to find the lower and upper bound for P_0.

The search is initialized with $P_0 = P_{res} - dp_{min}$, where dp_{min} is a tiny pressure (1 Pa). If this point does not yield a valid integration then dp is increased tenfold and the new point $P_0' = P_0 - dp$ is tested. The process is repeated until a valid starting point has been found; to prevent too coarse step-sizes, dp is not increased beyond an upper bound of 1 bar. This method cannot guarantee that a valid point is found (in fact no method can guarantee this); however in the practical examples studied this strategy has always found a valid point.

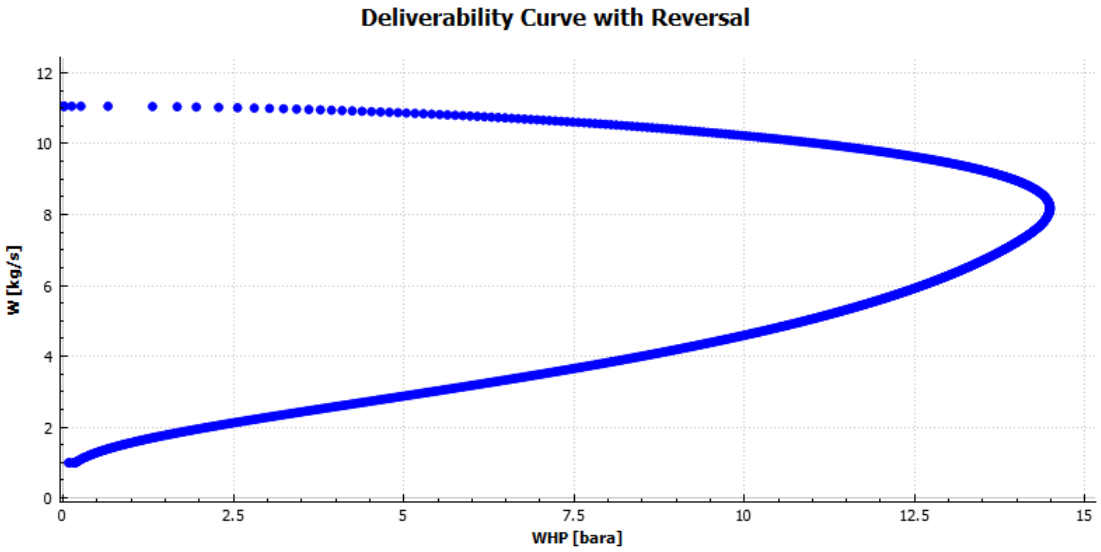

Figure 2: A full wellhead deliverability curve for a well with one feedzone. The upper section belongs to the high flow part where P_0 tends towards zero. The lower section belongs to the part where P_0 approaches P_{res}. The curve in this particular example shows a full reversal, i.e. the search algorithm must recognize this else it might only generate a small part of the lower section. In practical application one is usually only interested in the upper section towards the MDP; the lower part is unstable because the two phase fluid column can separate and collapse.

Once the starting point has been found a divide-and-conquer algorithm is started where the case $P_0 \rightarrow 0$ is investigated to find the lower bound for P_0 which has a sufficiently low wellhead pressure $WHP < WHP_{min}$. WHP_{min} is a user defined setting and typically just below a minimum separator pressure requirement. The algorithm is robust enough to deal with very small values of WHP_{min} (~0.01 bar); it becomes computationally more expensive to use lower settings. Figure 1 shows an example where the lower bound of P_0 just reaches the wellhead without turning into invalid conditions.

Care must be taken to identify cases where the deliverability curve shows a reversal, i.e. where the wellhead pressure increases temporarily with decreasing P_0. If such a case is encountered then P_0 must be lowered further even if the wellhead pressure is already below WHP_{min} in order to fully complete the deliverability curve.

After the lower bound for P_0 has been found the search is turned around and the upper bound is found by investigating $P_0 \rightarrow P_{res}$. This is a low-flow case that usually does not give many problems for single feedzone cases. However due to the discrete nature of the integration algorithm it is possible that the heat conduction term removes or adds too much heat in a single integration step and the enthalpy can potentially move outside the valid region of the thermodynamic table. The search $P_0 \rightarrow P_{res}$ hence determines the minimum flow rate where the integration still yields a valid result. Figure 1 shows such a case where the upper bound for P_0 differs significantly from P_{res}.

With both lower and upper bound for P_0 found the algorithm can step through the valid domain to complete the deliverability curve by dividing the range into a specified number of equally spaced points.

4.3. Multiple Feedzones

In the single feedzone case, the integration from the bottom feedzone upwards will only fail due to invalid thermodynamic conditions. When multiple feedzones are involved the situation becomes more complex and some additional issues need to be considered.

The first problem is that the upper feedzones can act as fluid loss zones and total loss of fluid is possible. Figure 3 shows such a case where the reservoir pressure at the upper feedzone is sufficiently low to draw all fluid from the wellbore. The solution to this "total loss" case is to further reduce the bottom hole pressure P_0; this will result in more fluid coming into the wellbore from the lower feedzones and less fluid loss in the higher feedzones. Hence this will influence the upper bound of P_0.

The next problem is that in some cases with $P_0 \rightarrow P_{res}$ (i.e. low-flow from the lower feedzones) there is still a positive pressure differential in the upper feedzones, i.e. they still act as fluid sources to the wellbore. This case can be further separated into two cases: an "extreme" case where the draw of fluid from the top zones is so heavy that the integration cannot reach the top due to high friction losses, and a more "benign" case where the integration reaches the wellhead but not with a flow rate tending towards zero.

In the extreme case it becomes necessary to abort integrating from the bottom feedzone upwards and to start the integration at the next feedzone upwards. These cases usually occur where a very prolific feedzone is located above a very poor feedzone; eliminating the bottom feedzone from the integration hence results in a small error in the total flow rate at the wellhead.

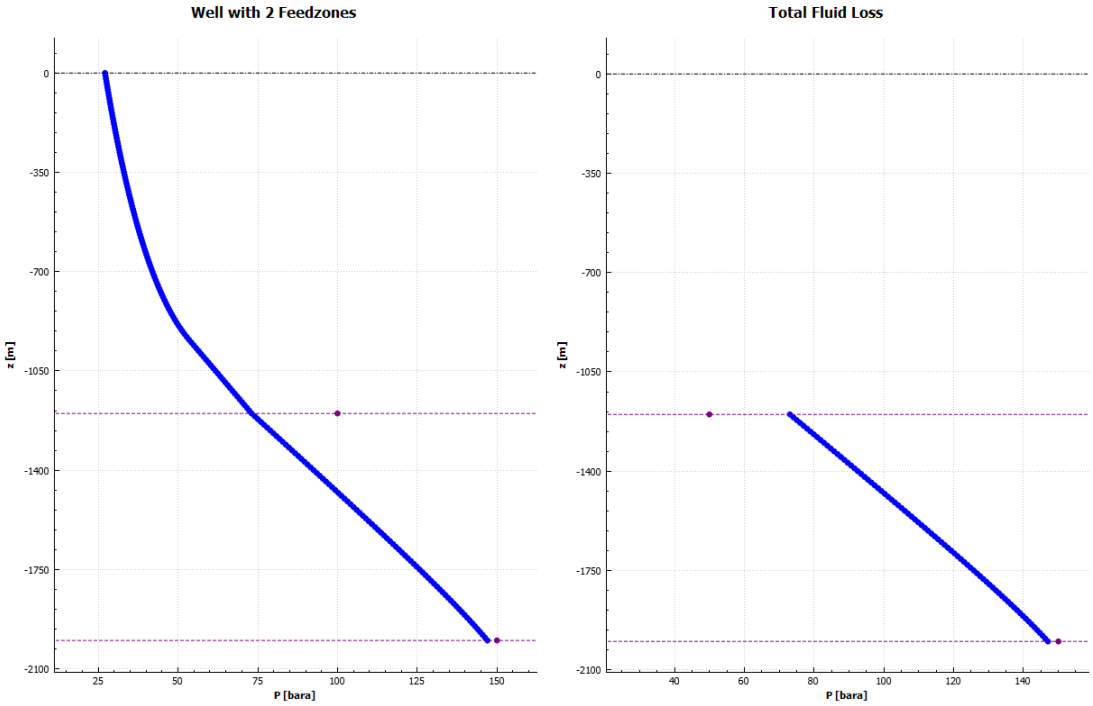

Figure 3: The left plot shows a well with two feedzones that both act as fluid sources. In the right hand plot the upper feedzone acts as a sink since the reservoir pressure is below the wellbore pressure. In the example shown the pressure difference is sufficient to draw all fluid from the wellbore, hence the integration cannot continue beyond the upper feedzone.

In the benign case it is possible to complete the deliverability curve by keeping the results from the simulation using the bottom feedzone, adding an addition to the simulation starting at the upper feedzone that still provided fluid; this usually results in a small bump in the deliverability curve since it ignores that fact the some of the fluid entering at the upper feedzone would actually travel down the wellbore towards the lower feedzones. However it is hard to define the specifics of this process; it is possible that two-phase flow would split and that liquid would travel downwards and steam upwards, for example. However since this process happens in the vicinity of the MDP of the deliverability curve, it is often permissible to simplify this process and allow all fluid gained to travel upwards; the resulting error will be small in absolute flow rate numbers. Figure 4 illustrates this case.

5. APPLICATIONS

5.1. Standalone Wellbore Simulator

Since its implementation Paiwera has been used at MRP as the standard tool for 1) modeling wellbore profiles using PTS data and 2) wellhead curves using data observed at the wellhead. The agreement with downhole data using sensible model parameters is usually excellent and often within the PTS instrument error. Wellhead data is often of poorer quality since mass flow rates and enthalpies are not directly measured with high frequency or over a wide operating rage; given this limitation the simulation results usually agree very well with the data.

5.2. Uncertainty Propagation

Given its robustness Paiwera is well suited to automated modeling tasks where input parameters vary over a wide range. Once sensible parameter ranges have been established it becomes possible to test the uncertainty propagation of these parameters to a desired observation.

Towards this end Paiwera can be linked with the iTOUGH2PEST program (Finsterle, 2011). Paiwera's graphical user interface can automatically generate, run and analyze iTOUGH2PEST files for simple tasks. As an add-on, the modeler can put the data generated through a simple plant model to investigate effects the model parameters have towards plant output. Figure 5 shows an example where the rugosity was sampled using a normal distribution.

5.3. Coupled Reservoir/Wellbore/Surface Simulator

The Paiwera C++ library can be used in combination with other reservoir and surface simulators to form a fully coupled reservoir-wellbore-surface facilities simulator. The first example was the OOMPFS code (Franz, 2015). Recently another fully coupled code was developed with assistance from John Burnell (GNS). This new code – T2OOMPFS – has been successfully used on existing TOUGH2 models and allows the modeler to create a complex surface network; plants can automatically allocate the mass flow required for their generation target. Combined with the coupled wellbore simulator it is now possible to create more realistic production/injection scenarios.

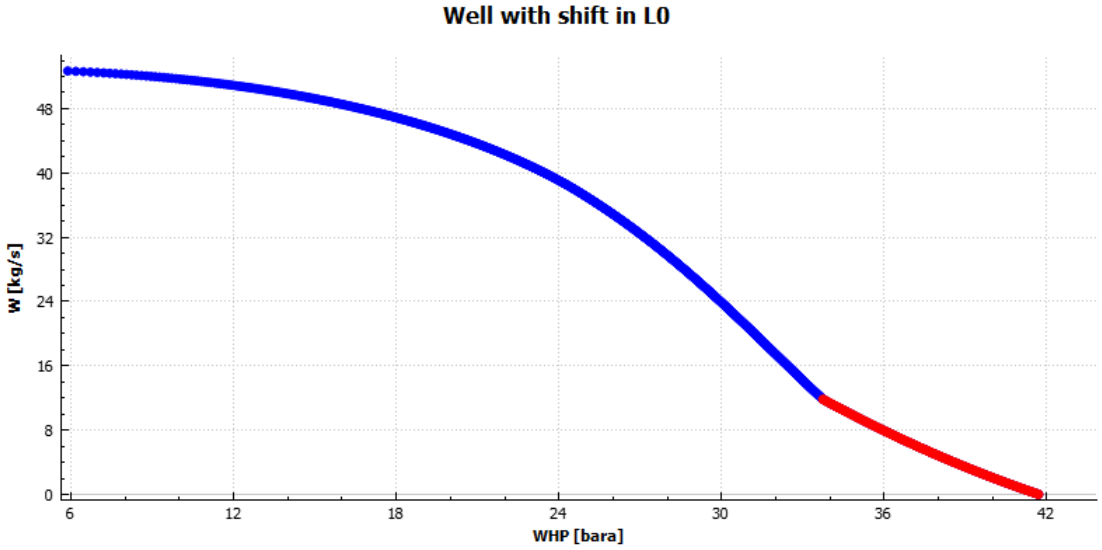

Figure 4: Well with two feedzones. With P_0 approaching P_{res} the upper feedzone is still over-pressured; to complete the deliverability curve the start of integration L_0 is shifted into the upper feedzone. The result is the small red section of the curve. This approach potentially overestimates the actual flow rate of the well; in reality some of the fluid could flow downwards towards the lower feedzone.

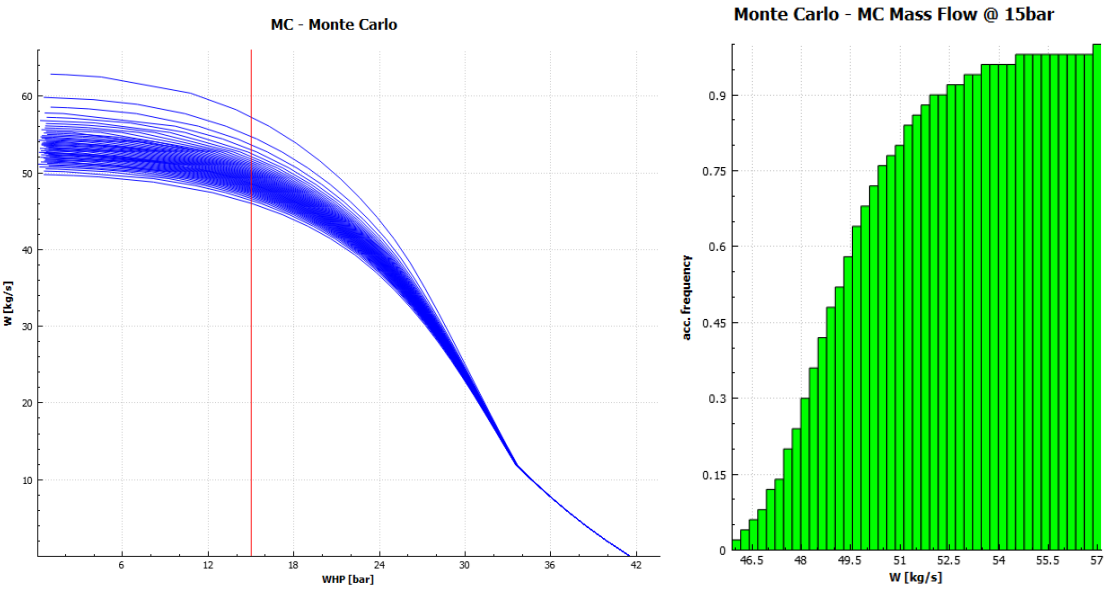

Figure 5: Example of a Monte Carlo simulation. The rugosity parameter was varied according to a normal distribution. The impact on the mass flow rate at the wellhead depends on the operating point of the well; the modeler can analyze a slice at a given wellhead pressure in the form of an S-curve or histogram.

SUMMARY

The search methods and thermodynamic tables described here allow the determination of the full operating range of a geothermal well. The wellbore simulator Paiwera has been used successfully at MRP on a variety of fields and on wells with very different designs and reservoir characteristics.

A very high number (>100,000) of model runs have been performed using fully coupled or Monte-Carlo modes. All investigated cases where Paiwera could not find a valid solution showed that the well would indeed be dead under the reservoir situation modeled. This underlines the robustness of the methods presented.

ACKNOWLEDGEMENTS

I would like to thank John Burnell (GNS) for his invaluable help with the coupling between Paiwera/OOMPFS and TOUGH2. Further I would like to thank Jan Beske for his assistance in coding the IAPWS97-IF steam tables.

REFERENCES

Aunzo, Z. P., Bjornsson, G., & Bodvarsson, G. S. (1991). *Wellbore Models GWELL, GWNACL, and HOLA User's Guide*. LBL-31428.

Battistelli, A., Calore, C., & Pruess, K. (1997). The Simulator TOUGH2/EWASG for Modelling Geothermal Reservoirs with Brines and Non-Condensible Gas. *Geothermics*, *26*(4), 437–464.

Carroll, J. J., Slupsky, J. D., & Mather, A. E. (1991). The Solubility of Carbon Dioxide in Water at Low Pressure. *J.Phys.Chem.Ref.Data.*, *20*(6), 1201–1209.

Duns, H., & Ros, N. C. J. (1963). Vertical flow of gas and liquid mixtures in wells. In *6th World Petroleum Congress* (pp. 451–465). World Petroleum Congress.

Ellis, A. J., & Golding, R. M. (1963). The Solubility of Carbon Dioxide above 100C in Water and in Sodium Chloride Solutions. *American Journal of Science*, *261*, 47–60.

Finsterle, S. (2011). *iTOUGH2 Universal Optimization Using the PEST Protocol User ' s Guide*. LBNL-3698E.

Franz, P. (2015). OOMPFS – A New Software Package for Geothermal Reservoir Simulation. *Proceedings World Geothermal Congress 2015* .

Hasan, A. R., & Kabir, C. S. (2002). *Fluid Flow and Heat Transfer in Wellbores*. Society of Petroleum Engineers.

Hasan, A. R., & Kabir, C. S. (2010). Modeling two-phase fluid and heat flows in geothermal wells. *Journal of Petroleum Science and Engineering*, *71*(1-2), 77–86. http://doi.org/10.1016/j.petrol.2010.01.008

IAPWS-IF97. (2007). *The International Association for the Properties of Water and Steam: Revised Release on the IAPWS Industrial Formulation 1997 for the Thermodynamic Properties of Water and Steam*. Lucerne, Switzerland.

Peter, P., & Acuna, J. A. (2010). Implementing Mechanistic Pressure Drop Correlations in Geothermal Wellbore Simulators. In *Proceedings World Geothermal Congress 2010*.

Press, W. H., Teukolsky, S. A., Vetterling, W. T., & Flannery, B. P. (2007). *Numerical Recipes* (3rd ed.). Cambridge University Press.

Pritchett, J. W., Rice, M. H., & Riney, T. D. (1981). *Equation-of-State for Water-Carbon Dioxide Mixtures: Implications for Baca Reservoir*.

Sutton, F. M., & McNabb, A. (1977). Boiling curves at Broadlands geothermal field, New Zealand. *New Zealand Journal of Science*, *20*, 333–337.